

C 344.1p + C 345k

20/8

H-86  
ОБЪЕДИНЕННЫЙ  
ИНСТИТУТ  
ЯДЕРНЫХ  
ИССЛЕДОВАНИЙ

Дубна

Nucl. Instr. & Meth., 1967,  
v. 99, N2, p. 229-234

E 13-2926



A.Z.Hryniewicz , S.Kopta ,  
S.Szymczyk , T.Walczak ,

EFFECTIVE RESOLVING TIME  
IN COINCIDENCE MEASUREMENTS  
ON THE CYCLOTRON BEAM

ЛАБОРАТОРИЯ ЯДЕРНЫХ РЕАКЦИЙ

1966

E13-2926

4540 / 1 up.  
A.Z.Hryniewicz<sup>x/</sup>, S.Kopta<sup>x/</sup>,  
S.Szymczyk<sup>x/</sup>, T.Walczak<sup>x/</sup>,

EFFECTIVE RESOLVING TIME  
IN COINCIDENCE MEASUREMENTS  
ON THE CYCLOTRON BEAM

Submitted to Nucl.Instr. and Meth.

---

<sup>x/</sup> Institute of Nuclear Physics, Cracow, Poland.

## 1. Introduction

The pulsation of the cyclotron beam complicates coincidence measurements and makes it difficult to determine the background of chance coincidences. In this case the effective resolving time of the coincidence set-up depends on different parameters and can be many times longer than the resolving time of the same coincidence circuit used for measurements with the continuously radiating source. This corresponds to a detrimental increase of the chance coincidence background.

The cyclotron beam consists of bunches of particles. Bunching frequency is equal to the high frequency on dees and the bunch width depends on the phase interval involved in the acceleration process. Typical figures for a bunching period and for a bunch width are 100 nsec and 10 nsec. In many machines the h f voltage on dees is modulated with the low frequency square pulses, the modulation frequency being of the order of 100 c/sec. The duty cycle of the cyclotron is determined as the ratio of h. f pulse duration to their repetition period. Both kinds of beam modulation should be taken into account when the effective resolving time of the coincidence circuit is to be calculated.

In coincidence measurements the fast coincidence circuit is fed by appropriately shaped, fast pulses from two detectors. We assume that these pulses have a rectangular shape and we denote their lengths by  $r_1$  and  $r_2$ . In most cases encountered in practice the electronic resolving time of the total coincidence circuitry is determined by the resolving time of the fast circuit. Only in the case of very high counting rates must higher order corrections be introduced involving the resolving time of a slow coincidence circuit and the dead time of single channel analysers and gating circuits<sup>/1/</sup>. When measurements with a source of continuous radiation are performed the resolving time is equal to the sum of the time widths of the two detector pulses  $r_1 + r_2$ .

In the case of a modulated source the average counting rate of chance coincidence can be expressed in the form

$$\langle N_{c1} \rangle = \langle N_1 \rangle \langle N_2 \rangle r_{eff}, \quad (1)$$

where  $\langle N_1 \rangle$  and  $\langle N_2 \rangle$  are average single counting rates in the two channels. The averages are taken over a time interval much longer than the source modulation period. Formula (1) can be regarded as a definition of the effective resolving time  $r_{eff}$ . It is in general longer than  $r_1 + r_2$ <sup>/2/</sup>.

In order to simplify the calculations we assume that h.f. bunches are of rectangular shape. We denote their period by  $T$  and their width by  $b$ . In the present state of pulse electronics, circuits giving shaped detector pulses shorter than 20 nsec are very easy to build. Therefore, we limit our considerations to the case when the detector pulse widths  $r_1$  and  $r_2$  are shorter than the time interval  $T - b$  between successive cyclotron bunches. This means that the adjacent cyclotron bunches do not contribute to the formation of chance coincidences.

We have to consider separately the case when the two detectors register no background between h.f. bunches and that one when some background is present. The first case corresponds to the detection of scattered particles or particles produced in nuclear reactions while the second one corresponds to the detection of gamma rays.

## 2. Calculations of the Effective Resolving Time

### 2.1. No background between cyclotron bunches.

In measurements with continuously radiating sources, the time interval in which two uncorrelated pulses must appear in order to produce a chance coincidence is equal to  $r_1 + r_2$  and is independent of the appearance time of

the first pulse. For a pulsed source, when  $b \leq r_1, r_2 \leq T - b$ , the time interval for the formation of a chance coincidence is determined by the cyclotron bunch width  $b$ . When  $r_1$  or  $r_2 < b$ , this time interval depends on the time distance of the detector pulses from the edge of the cyclotron bunch.

For a source of continuous radiation the introduction of delay in one channel of the coincidence circuit does not change the chance coincidence counting rate. For a pulsed source the chance coincidence counting rate determination as a function of delay gives a "delayed chance coincidence curve", whose shape and width depend on the detector pulse lengths  $r_1$  and  $r_2$  and on the bunch width  $b$ . In other words, the introduction of delay changes the effective resolving time of the coincidence circuit.

In order to calculate the effective time let us assume that during the cyclotron bunch the counting rate in channel 1 is  $N_1$ . Then the average counting rate of chance coincidences  $\langle N_{ch} \rangle$  can be written in the form

$$\langle N_{ch} \rangle = \frac{N_1}{T} \int_0^b f(t) dt, \quad (2)$$

where  $f(t)$  represents the probability that the pulse appearance at the time  $t$  in channel 1 will be accompanied by the pulse in channel 2 in such a time interval that the coincidence circuit will register a chance coincidence.

If channel 2 is fed by pulses from a continuously radiating source, the function  $f(t)$  would be independent of time and it would have the form  $N_2(r_1 + r_2)$ , where  $N_2$  is the counting rate in channel 2. When the detector pulses in channel 2 are also modulated, the function  $f(t)$  can be written in the form

$f(t) = N_2 g(t)$ , where  $N_2$  is now the counting rate in channel 2 during the cyclotron bunch.  $g(t)$  has the physical meaning of the time interval given, by the appearance at the time  $t$  of the pulse in channel 1, to pulses from channel 2 for the formation of a chance coincidence. The average chance coincidence counting rate takes the form

$$\langle N_{ch} \rangle = \frac{N_1 N_2}{T} \int_0^b g(t) dt. \quad (3)$$

The function  $g(t)$  depends on the position of the time  $t$  in respect to the edge of the cyclotron bunch and on the lengths of pulses  $r_1$  and  $r_2$ .

Comparing the formula (3) with the formula (1) and using the relations

$$\langle N_1 \rangle = N_1 \frac{b}{T} \quad \text{and} \quad \langle N_2 \rangle = N_2 \frac{b}{T}$$

we get

$$r_{eff} = \frac{T}{b^2} \int_0^b g(t) dt . \quad (4)$$

Calculation of the effective resolving time reduces to the determination of the integral  $\int_0^b g(t) dt$ . In order to do this we have to divide the cyclotron bunch (time interval / 0, b /) into appropriate subintervals and to calculate the  $g(t)$  dependence for them.

For the special case of  $r_2 \leq r_1 \leq b$ ,  $r_1 + r_2 \geq b$  the shape of  $g(t)$  is shown in Fig. 1. Only for  $b - r_1 \leq t \leq r_2$  has the function  $g(t)$  the constant value  $g(t) = b$ , which means that the time interval for the formation of a chance coincidence is equal to the full bunch width. For  $-r_1 \leq t \leq b - r_1$   $g(t) = r_1 + t$  and for  $r_2 < t < b + r_2$   $g(t) = b + r_2 - t$ . The shaded area in Fig. 1 represents, then, the value of the integral in the formula (4).

For different lengths of the detector pulses  $r_1$  and  $r_2$  in respect to the cyclotron bunch width  $b$  the integration limits  $(0, b)$  overlap different parts of the variability range  $(-r_1, b + r_2)$  of the function  $g(t)$  and different special cases must be considered separately.

When  $r_1 + r_2 \leq b$  the limits of the subinterval  $(b - r_1, r_2)$  (see Fig. 1) are interchanged and the  $g(t)$  value for  $r_2 < t < b - r_1$  is equal to  $r_1 + r_2$ .

The introduction of delay  $d$  to one of the pulse channels corresponds to the time scale shift by  $d$ . New subinterval limits and the corresponding  $g(t)$  values can be calculated for the delay  $d_1$  in channel 1 by replacing  $t$  by  $t + d_1$  and for the delay  $d_2$  in channel 2 by replacing  $t$  by  $t - d_2$ .

In the Table 1 the results of calculations of  $r_{eff}$  for different cases are given.

Figs. 2 and 3 show examples of "delayed chance coincidence curves" for cases 1A and 3. The curves are symmetrical and their centres are shifted by  $d_2 = b(r_1 - r_2)/2$  in respect to  $t = 0$ . The curve widths at the base are equal to  $r_1 + r_2 + 2b$ . In cases 2B and 3 they have plateau of the length  $r_1 + r_2 - 2b$ .

It can be seen from Table 1 that in case 3, the most frequently encountered in practice, the effective resolving time is independent of the lengths of detector pulses and is equal to the h.f. cyclotron period  $T / |3/x|$ .

<sup>x/</sup> It is important to bear in mind that this statement is true when the condition  $r_1, r_2 \leq T - b$  is fulfilled.

T a b l e 1

| Case                    | Delay                           | $r_{\text{eff}} \frac{b^2}{T}$                                      |
|-------------------------|---------------------------------|---------------------------------------------------------------------|
| 1A. $r_2 \leq r_1$ ,    | $0 \leq d_1 \leq r_2$           | $(r_1 + r_2) b - \frac{1}{2}(r_1^2 + r_2^2) + d_1(r_2 - r_1 - d_1)$ |
| $r_1 + r_2 \leq b$ .    | $r_1 \leq d_1 \leq b - r_2$     | $(r_1 + r_2) [b - d_1 - \frac{1}{2}(r_1 - r_2)]$                    |
|                         | $b - r_1 \leq d_1 \leq b + r_2$ | $\frac{1}{2}(b + r_2 - d_1)^2$                                      |
| 1B.                     | $0 \leq d_1 \leq b - r_1$       | $(r_1 + r_2) b - \frac{1}{2}(r_1^2 + r_2^2) + d_1(r_2 - r_1 - d_1)$ |
| $r_2 \leq r_1 \leq b$ , | $b - r_1 \leq d_1 \leq r_2$     | $\frac{1}{2}(b + r_2 - d_1)^2 - (r_2 - d_1)^2$                      |
| $r_1 + r_2 \geq b$ .    | $r_2 \leq d_1 \leq b + r_2$     | $\frac{1}{2}(b + r_2 - d_1)^2$                                      |
| 2A.                     | $0 \leq d_1 \leq r_2$           | $\frac{1}{2}(b + r_2 - d_1)^2 - (r_2 - d_1)^2$                      |
| $r_2 \leq b \leq r_1$ , | $r_2 \leq d_1 \leq b + r_2$     | $\frac{1}{2}(b + r_2 - d_1)^2$                                      |
| $r_1 + r_2 \leq 2b$ ,   | $0 \leq d_2 \leq r_1 - b$       | $\frac{1}{2}(b + r_2 + d_2)^2 - (r_2 + d_2)^2$                      |
| $r_1 \leq T - b$ .      | $r_1 - b \leq d_2 \leq b - r_2$ | $(r_1 + r_2) b - \frac{1}{2}(r_1^2 + r_2^2) + d_2(r_1 - r_2 - d_2)$ |
|                         | $b - r_2 \leq d_2 \leq r_1$     | $\frac{1}{2}(b + r_1 - d_2)^2 - (r_1 - d_2)^2$                      |
|                         | $r_1 \leq d_2 \leq b + r_1$     | $\frac{1}{2}(b + r_1 - d_2)^2$                                      |
| 2B.                     | $0 \leq d_1 \leq r_2$           | $\frac{1}{2}(b + r_2 - d_1)^2 - (r_2 - d_1)^2$                      |
| $r_2 \leq b \leq r_1$ , | $r_2 \leq d_1 \leq b + r_2$     | $\frac{1}{2}(b + r_2 - d_1)^2$                                      |
| $r_1 + r_2 \geq 2b$ ,   | $0 \leq d_2 \leq b - r_2$       | $\frac{1}{2}(b^2 - r_2^2 + d_2^2) + b r_2$                          |
| $r_1 \leq T - b$        | $b - r_2 \leq d_2 \leq r_1 - b$ | $b^2$                                                               |
|                         | $r_1 - b \leq d_2 \leq r_1$     | $\frac{1}{2}(b + r_1 - d_2)^2 - (r_1 - d_2)^2$                      |
|                         | $r_1 \leq d_2 \leq b + r_1$     | $\frac{1}{2}(b + r_1 - d_2)^2$                                      |
| 3.                      | $0 \leq d_1 \leq r_2 - b$       | $b^2$                                                               |
| $b \leq r_2 \leq r_1$   | $r_2 - b \leq d_1 \leq r_2$     | $\frac{1}{2}(b + r_2 - d_1)^2 - (r_2 - d_1)^2$                      |
| $r_1 \leq T - b$        | $r_2 \leq d_1 \leq b + r_2$     | $\frac{1}{2}(b + r_2 - d_1)^2$                                      |
|                         | *)                              |                                                                     |

x/ The case of delay in channel 2 corresponds to the interchange of indices 1 and 2.



## 2.2. Background between cyclotron bunches

When the detectors register some background between the cyclotron bunches three additional terms must be introduced to the chance coincidence formula. They represent chance coincidences of pulses from the cyclotron bunch with background pulses and chance coincidences of background-background pulses.

$$\begin{aligned} \langle N_{\sigma h} \rangle = & \langle N_1 \rangle \langle N_2 \rangle r_{\text{eff}} + \langle N_1 \rangle N_2' (r_1 + r_2) + \\ & + \langle N_2 \rangle N_1' (r_1 + r_2) + N_1' N_2' (r_1 + r_2). \end{aligned} \quad (5)$$

$r_{\text{eff}}$  is the effective resolving time calculated in the previous paragraph and the meaning of other notations is illustrated in Fig. 4.

The expression for the average chance coincidence counting rate can be written in another form

$$\langle N_{\sigma h} \rangle = \langle N_1^B \rangle \langle N_2^B \rangle r_{\text{eff}}^B \quad (6)$$

introducing the new resolving time  $r_{\text{eff}}^B$  and the average counting rates in the two channels  $\langle N_1^B \rangle = \langle N_1 \rangle + N_1'$  and  $\langle N_2^B \rangle = \langle N_2 \rangle + N_2'$ .

Using the relations

$$\langle N_1 \rangle = \frac{b}{T} N_1 \quad \text{and} \quad \langle N_2 \rangle = \frac{b}{T} N_2$$

and comparing the formulae (5) and (6) we find

$$r_{\text{eff}}^B = \frac{\theta^2 r_{\text{eff}} + (r_1 + r_2)(\eta_1 \theta + \eta_2 \theta + \eta_1 \eta_2)}{(\theta + \eta_1)(\theta + \eta_2)}, \quad (7)$$

where

$$\theta = \frac{b}{T}, \quad \eta_1 = \frac{N_1'}{N_1} \quad \text{and} \quad \eta_2 = \frac{N_2'}{N_2}.$$

When the detector 1 does not register any background  $\eta_1 = 0$  and

$$r_{\text{eff}}^B = \frac{\theta r_{\text{eff}} + \eta_2 (r_1 + r_2)}{\theta + \eta_2} \quad (8)$$

if additionally  $b \leq r_1, r_2 \leq T - b$  then  $r_{\text{eff}} = T$  and

$$r_{\text{eff}}^B = \frac{b + \eta_2 (r_1 + r_2)}{\theta + \eta_2} \quad (9)$$



The last formula is identical with that obtained by J. Mössner et al. / 4/ .

When the background contribution increases,  $r_{\text{eff}}^B$  decreases from  $T$  to  $r_1 + r_2$  . For measurements with a continuously radiating source ( $\eta_1 = \eta_2 = \infty$ )  $r_{\text{eff}}^B$  reduces to  $r_1 + r_2$  .

### 2.3. Role of the cyclotron duty cycle.

A cyclotron duty cycle  $D$  lower than 1 leads to further increase in the effective resolving time. As the l.f. cyclotron pulses have a length of 1 msec or more, the edge effects can be neglected in our considerations.

We assume at first that the background between l.f. cyclotron pulses is constant and that its value is the same as that between the h.f. bunches. Then the average chance coincidence counting rate

$$\begin{aligned} \langle N_{\text{oh}} \rangle = & \frac{1}{S} \langle N_1 \rangle \langle N_2 \rangle r_{\text{eff}} + \frac{1}{S} \langle N_1 \rangle N_2' (r_1 + r_2) + \\ & + \frac{1}{S} \langle N_2 \rangle N_1' (r_1 + r_2) + N_1' N_2' (r_1 + r_2) , \end{aligned} \quad (10)$$

where  $S = 1/D$ . Introducing average counting rates in both channels

$$\langle N_1^* \rangle = \frac{1}{S} \langle N_1 \rangle + N_1' \quad \text{and} \quad \langle N_2^* \rangle = \frac{1}{S} \langle N_2 \rangle + N_2'$$

we can write according to the definition of the effective resolving time (1)

$$\langle N_{\text{oh}} \rangle = \langle N_1^* \rangle \langle N_2^* \rangle r_{\text{eff}}^* , \quad (11)$$

where  $r_{\text{eff}}^*$  is a new effective resolving time. Comparison of the formulae (10) and (11) gives

$$r_{\text{eff}}^* = S \frac{\theta r_{\text{eff}} + (r_1 + r_2) (\eta_1 \theta + \eta_2 \theta + S \eta_1 \eta_2)}{(\theta + S \eta_1) (\theta + S \eta_2)} . \quad (12)$$

In the case when the detector 1 does not register any background  $\eta_1 = 0$

$$r_{\text{eff}}^* = S \frac{\theta r_{\text{eff}} + \eta_2 (r_1 + r_2)}{\theta + S \eta_2} . \quad (13)$$

For  $b \ll r_1, r_2 \ll T - b$   $r_{\text{eff}} = T$  and

$$r_{\text{eff}}^* = S \frac{b + \eta_2 (r_1 + r_2)}{\theta + S \eta_2} . \quad (14)$$

If there is now background in either detector ( $\eta_1 = \eta_2 = 0$ )

$$r_{\text{eff}}^{\text{B}} = ST \quad . \quad (15)$$

The most general case considered by us is that when the background  $N_1''$  and  $N_2''$  between h.f. cyclotron pulses is constant but different from the background  $N_1'$  and  $N_2'$  between h.f. bunches. Let us denote by  $p_1$  and  $p_2$  the ratios of the two background levels in channels 1 and 2

$$p_1 = \frac{N_1''}{N_1'} \quad \text{and} \quad p_2 = \frac{N_2''}{N_2'} \quad .$$

Then

$$\begin{aligned} \langle N_{\text{ch}} \rangle &= \langle N_1^{\text{B}P} \rangle + \langle N_2^{\text{B}P} \rangle + r_{\text{eff}}^{\text{B}P} = \\ &= \left[ \frac{1}{S} \langle N_1^{\text{B}} \rangle + \left(1 - \frac{1}{S}\right) N_1'' \right] \left[ \frac{1}{S} \langle N_2^{\text{B}} \rangle + \left(1 - \frac{1}{S}\right) r_{\text{eff}}^{\text{B}P} \right] = \\ &= \frac{1}{S} \langle N_1^{\text{B}} \rangle + \langle N_2^{\text{B}} \rangle + r_{\text{eff}}^{\text{B}} + \left(1 - \frac{1}{S}\right) N_1'' N_2'' (r_1 + r_2) , \end{aligned} \quad (16)$$

hence

$$r_{\text{eff}}^{\text{B}P} = S \frac{\theta^2 r_{\text{eff}}^{\text{B}} + (r_1 + r_2) [\theta(\eta_1 + \eta_2) + \eta_1 \eta_2 [1 + p_1 p_2 (S - 1)]]}{\{\theta + \eta_1 [1 + p_1 (S - 1)]\} \{\theta + \eta_2 [1 + p_2 (S - 1)]\}} \quad . \quad (17)$$

It is easy to prove that the last formula includes all the more special cases considered before.

### 3. Experimental Check of the Theoretical Considerations

The formulae given above were obtained using the following assumptions, which might limit their application in the experimental work:

- a) stability of the cyclotron current,
- b) rectangular shape of the cyclotron bunches,
- c) rectangular shape of the detector pulses ,
- d) constant background between cyclotron pulses.

In order to check the influence of the shape of the cyclotron bunches we performed calculations for the different bunch shapes illustrated in Fig. 5. It appeared that only the slope of the delayed chance coincidence curve is affected, its plateau length and its base width being unchanged.

The time dependence of the background between bunches, due to the for-

mation of short-lived activities, with the life time comparable or shorter than the bunching period  $T$ , will cause some broadening and asymmetry of the delay chance coincidence curve.

The simplest experimental method of chance coincidence rate determination is to introduce the delay  $T$  (equal to the bunching period) into one of the two channels. The coincidence spectrum taken in this way is pure chance coincidence spectrum unless some activity with the decay period comparable to  $T$  is produced during the investigated process. By splitting one channel into two parts and introducing the delay  $T$  in one of them, the chance coincidence and the total coincidence spectra can be obtained simultaneously. The subtraction gives the true coincidence spectrum regardless of any instability of the cyclotron current<sup>5/</sup>.

The possibility of determination of the cyclotron bunch width from the delayed chance coincidence curve was checked at the heavy ion cyclotron U-150 of the Laboratory of Nuclear Reactions, Joint Institute for Nuclear Research in Dubna. In the course of the coulomb excitation measurements on  $Pb^{208}$  described elsewhere<sup>6/</sup> the delayed chance coincidence curve for scattered particle-gamma detection was taken. The measurements were performed for such part of the gamma spectrum in which the true coincidence counting rate is quite negligible. Therefore, the introduction of the additional delay  $T$  was not needed and the two detectors counted pulses corresponding to the same cyclotron bunch.

The obtained curve is shown in Fig. 6. Shaped detector pulses of the length  $\tau = \tau_1 = \tau_2 = 20$  nsec were used. Knowing  $\tau$  it is possible to determine the cyclotron bunch width from the plateau or from the base lengths of the experimental curve. In Fig. 6 six theoretical curves are drawn for  $b = (5-9)$  and 10 nsec. The experimental points coincide satisfactorily with the curve for 8 nsec.

In our experimental case the parameters appearing in the formula (17) have the following values:

$$S = 4.35, \quad \theta = 0.073, \quad r_{off} = T = 110 \text{ nsec}$$

$$\eta_1 = 0.04, \quad \eta_2 = 0, \quad p_1 = 0.34, \quad p_2 = 0$$

where  $\theta$ ,  $\eta_1$ , and  $p_1$ , estimation was performed using  $b = 8$  nsec. These parameters give for zero delay  $r_{off}^{*p} = 265$  nsec what has to be compared with the electronic resolving time  $2\tau = 40$  nsec.

#### 4. C o n c l u s i o n s

The considerations concerning the effective resolving time show clearly the disadvantage of coincidence measurements at the cyclotrons when compared with measurements at the tandem generators.

The described delayed chance coincidence method proved to be useful for the determination of the cyclotron bunch width.

#### A c k n o w l e d g m e n t s

The authors express their deep gratitude to Professor G.N.Flerov for his constant interest in this work and valuable comments. It is a pleasure to acknowledge the cooperation of the cyclotron operating crew under engineer B.A.Za-ger.

#### R e f e r e n c e s

1. E.B.Shera, K.J.Casper, B.L.Robinson, Nucl.Instr. and Meth., 24, 482(1963).
2. N.Feather, Proc.Cambr.Phil.Soc., 45, 648 (1949).
3. M.Crut, D.R.Sweetman, N.S.Wall, Nuclear Phys., 17, 655 (1960).
4. J.Mösner, L.Pocs, J.Zimányi, Z.f.K.-Ph A6, Dezember 1962.
5. H.J.Hausman, G.F.Dell, H.F.Bowsher, Phys.Rev., 118, 1237 (1960).
6. A.Z.Hryniewicz, S.Kopta, S.Szymczyk, T.Walczak, I.Kuzniecov, Nuclear Phys., 79, 495 (1966).

Received by Publishing Department  
on September 13, 1966.

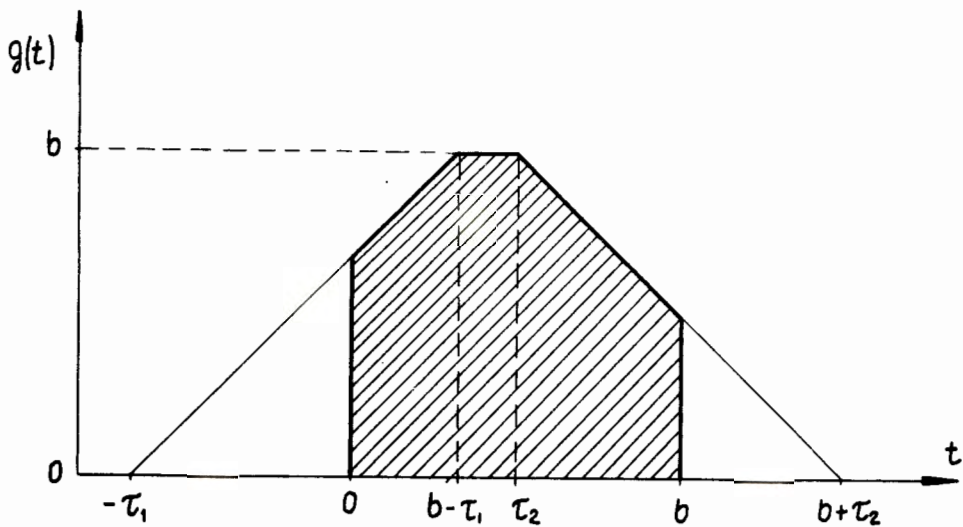


Fig. 1. Shape of the function  $g(t)$  for the case of  $r_2 < r_1 < b$ ,  $r_1 + r_2 > b$ .

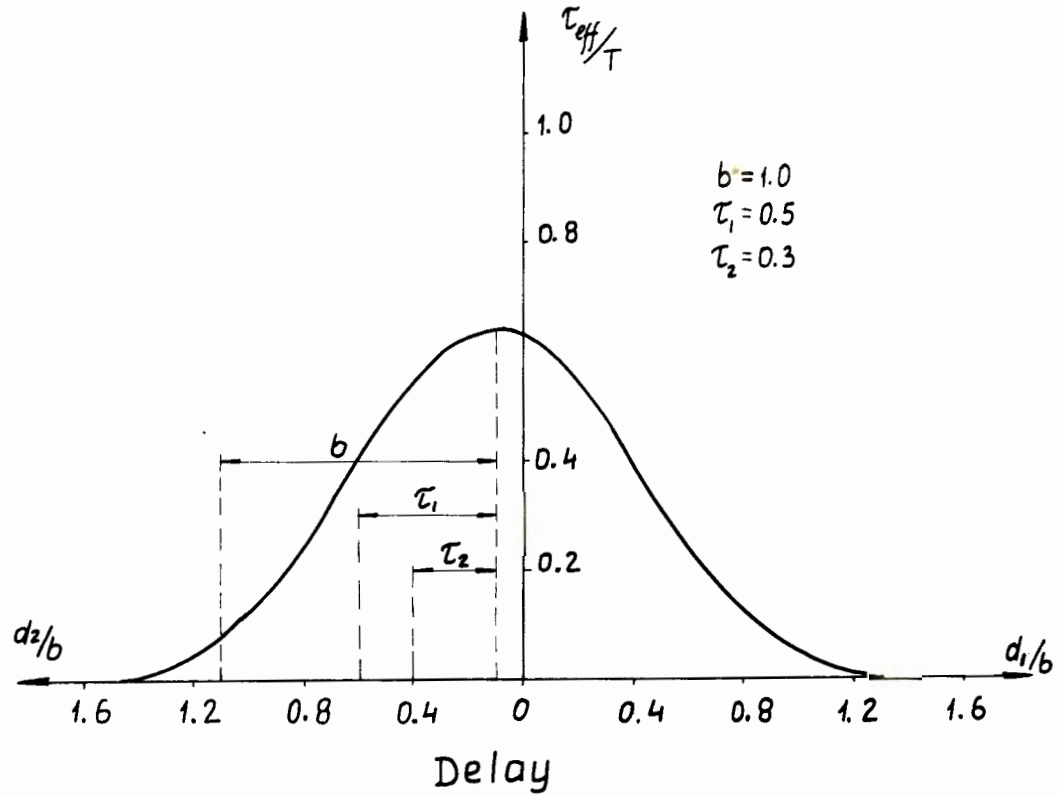


Fig. 2. Delayed chance coincidence curve for the case 1A.

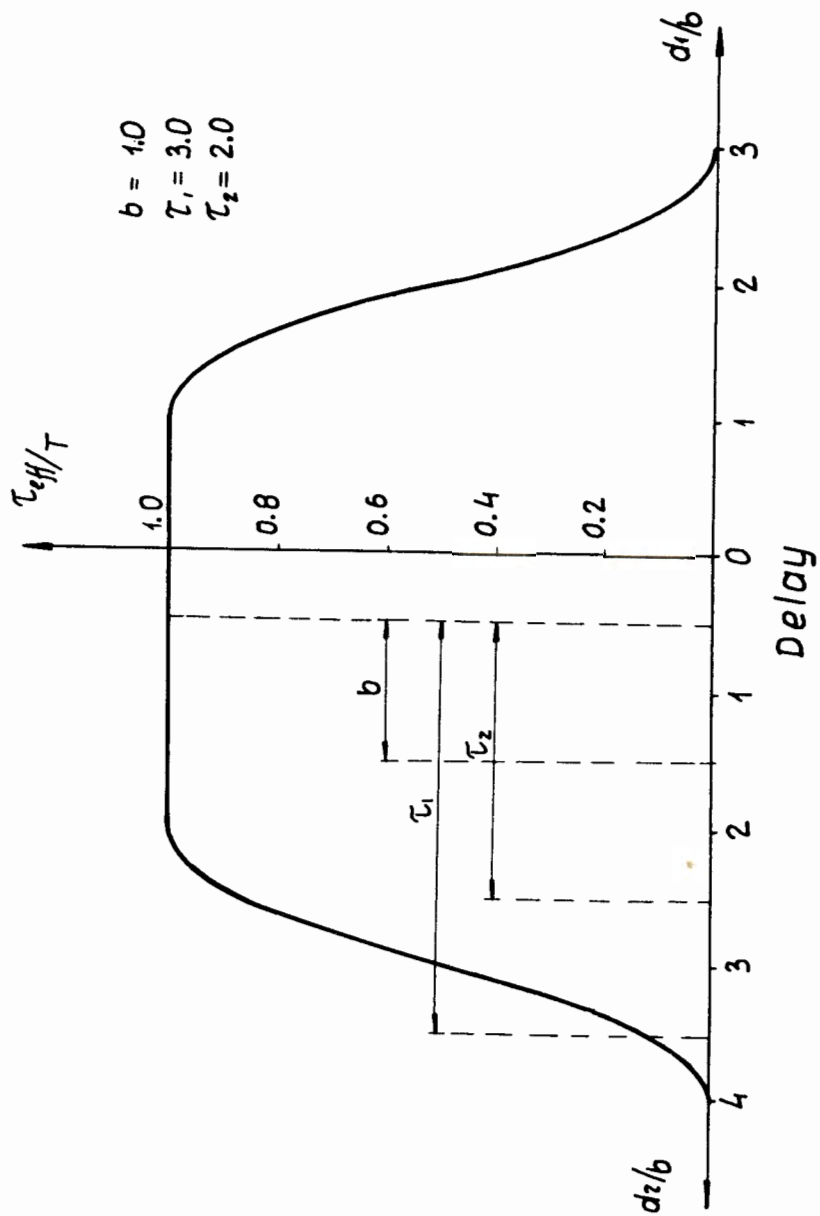


Fig. 3. Delayed chance coincidence curve for the case 3.



Fig. 5. Different postulated bunch shapes.

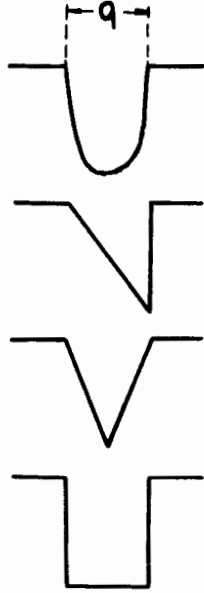
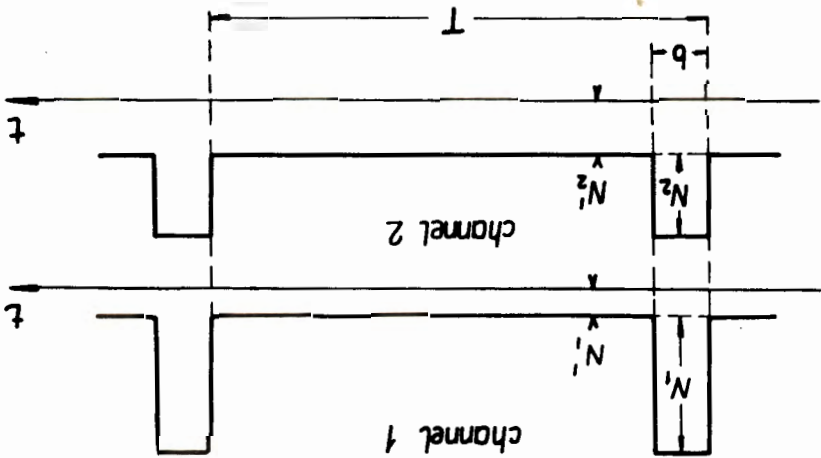
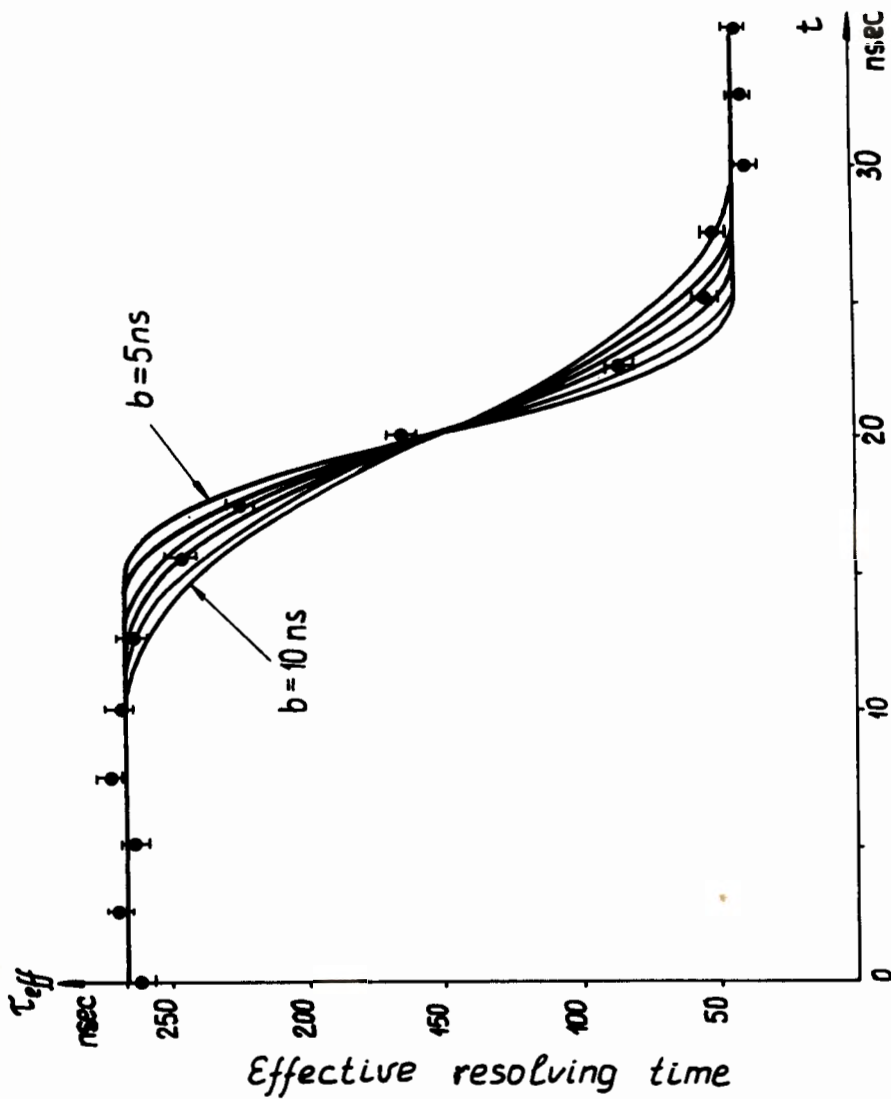


Fig. 4. Meaning of notations in the formula (5).





Delay time

Fig. 6. Experimental curve of delayed chance coincidences compared with theoretical curves for different values of  $b$ .